IEEE Access
Multidisciplinary | Rapid Review | Open Access Journal

Received September 20, 2019, accepted October 15, 2019, date of publication October 18, 2019, date of current version November 5, 2019.

Digital Object Identifier 10.1109/ACCESS.2019.2948261

Extending Velocity Sensor Bandwidth by Compensating Temperature Dependency Based on BP Neural Network

BO ZHAO, WEIJIA SHI, DING SUN, JIAXIN LI, FENG LI, AND JIUBIN TAN

Center of Ultra-Precision Optoelectronic Instrument Engineering, Harbin Institute of Technology, Harbin 150080, China
Key Lab of Ultra-Precision Intelligent Instrumentation, Ministry of Industry and Information Technology, Harbin Institute of Technology, Harbin 150080, China

Corresponding author: Weijia Shi (shiweijia@hit.edu.cn)

This work was supported in part by the National Major Scientific Instruments and Equipment Development Special Funds of China under Grant 2018YFF01012003.

ABSTRACT A compensation method for a magnetoelectric velocity sensor (MVS) is always necessary, which can lower the resonance frequency of the measuring system and subsequently extend the measuring bandwidth. In this paper, a novel compensation method is proposed based on the BP neural network under the TensorFlow architecture. Comparing with the existing methods, the new method does not depend upon an accurate model of the MVS any more, whose parameters are badly influenced by the temperature. The dynamic compensator is connected with the sensor. The BP neural network algorithm is used to identify compensation parameters. The dynamic compensator works at state of the optimum parameter all the time to compensate the dynamic performance of MVS by training the weights and thresholds of the neural network. The experiment results show that velocity measurement deviation is within ±5% error band by the dynamic compensator, which can reduce the measurement deviation caused by the variation of temperature and improve the measurement accuracy. The bandwidth can be as low as 0.28Hz. The dynamic compensator is superior to Random Forests and RBF Neutral Network in implement in FPGA/CPLD. Its' accuracy is superior to zero-pole compensation method. This method leads a new way to weaken the temperature variation characteristics of the velocity sensor and improve the measurement performance.

INDEX TERMS Velocity sensor, bandwidth expansion, temperature dependence, BP neural network.

I. INTRODUCTION

Vibration isolation systems are widely used in high-precision applications to achieve the extreme demands of accuracy [1]–[4]. The measurements of the vibration signal are very important for the active vibration isolation system [5], only based on which the closed-loop isolating system can be constructed. The output signal of absolute velocity sensor, such as the magnetoelectric velocity sensor (MVS) which has low output impedance and high sensitivity, comes from the relative motion between the inertia mass block and the outer shell [6]. In order to measure the ultra-low frequency signal, it is necessary to decrease the natural frequency of the detecting system and subsequently expand its bandwidth.

In vibration isolation search area, the frequency expansion technology of the MVS has attracted increasing attention of researchers in the precision engineering, such as the nano-scale measuring, the semiconductor manufacturing and the space exploring. The zero-pole compensation method is the widely-applied method to lower the natural frequency of the MVS, which is expected to cancel the natural pole of the transfer function of the sensor by introducing the carefully-designed zero of the compensation network [7], [8]. Then the designed pole of the compensation network acts as the pole of the whole detecting system, which is consisted by the sensor and the additional compensating network. Then, the new center frequency of the detecting system could be lower than before, which will match the system requirement [9].

In recent years, many ground simulators in aerospace field require vibration isolation foundation (VIF) with high integration and low frequency isolation performance. The MVSs are embedded in the platform of the VIF. The cooling equipment cannot be used to avoid additional disturbance from introducing external disturbance any more, such as

The associate editor coordinating the review of this manuscript and approving it for publication was Muhammad Imran Tariq.

the water flow. So the local temperature rising around the MVS during long-time running cannot be suppressed by the environmental control system. The temperature rise of the MVS will subsequently cause the parameters change, such as the natural frequency, the damping ratio, the sensitivity, and the frequency characteristic. So the existing compensation network will be ineffective because of the temperature dependence of the MVS.

There are two methods for sensor temperature compensation. The traditional method is hardware compensation, such as bridge method, negative temperature coefficient platinum resistance method [10], [11]. Because the resistance and capacitance parameters of hardware circuit are difficult to adjust and the flexibility is bad, software compensation is more frequently-used. Software compensation divides into two ways: modern filter and machine learning. Frequently-used modern filters include adaptive filtering algorithm [12]–[15] and Kalman filter [16], [17]. The adaptive filtering based on the Least Mean Square (LMS) is generally suitable for on-line identification of the system and it needs a reference signal. So it is not suitable for the MVS because the ideal output signal is unknown during the measurement process. The Kalman filter does not need ideal output signal as a reference, which is generally applicable to the signal to be filtered including other noise signals. But the temperature variation causes the change of the system transfer function, so the Kalman filter is also unsuitable. Machine learning includes RNN (Recurrent Neutral Network), CNN (Convolutional Neural Network), Random Forests, REF Neutral Network, SVM (support vector machines) and BP Neutral Network etc. The LSTM (Long Short-Term Memory) is a typical RNN neutral network structure. It has memory feature and is suitable for NLP (Natural Language Processing) with context [18]. But the output of MVS at any time is disturbed when temperature changes. So in the above case, LSTM may not suitable. And CNN has the ability of representation learning and can classify input information according to its hierarchical structure. It is mainly used for image recognition. Its' nonlinear mapping ability is less than BP neural network [19]. The RBF neural network is a typical local approximation network and it can approximate arbitrary continuous function with arbitrary precision. But RBF has only one hidden layer. Therefore, when training samples increase, the number of hidden neurons in RBF network is much higher than that of BP, which makes the complexity and structure of RBF network greatly increased, and the amount of computation also increased and it's also difficult to be implemented in FPGA/CPLD [20]. Because temperature compensation involves multiple frequency points in this paper, the training sample data is huge. So RBF is inappropriate. SVM is similar to the above. Random Forests are able to process high-dimensional data without feature selection with high training speed [21], [22]. But there will be over fitting for classification problems with large noise. Furthermore, Random Forest Algorithms are usually implemented in R Language and is so hard to implement in FPGA/CPLD based it's high processing speed. BP Neutral Network can be multiple hidden layers and we can adjust learning rate dynamically to improve the convergence rate. And It's easy to implement in FPGA/CPLD by matrix operation in VHDL (Very High Speed Integrated Circuit Hardware Description Language) or Verilog.

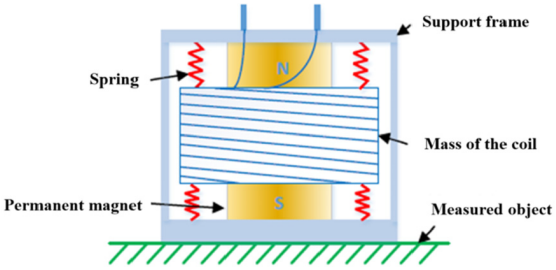

FIGURE 1. Mechanical structure sketch of the MVS.

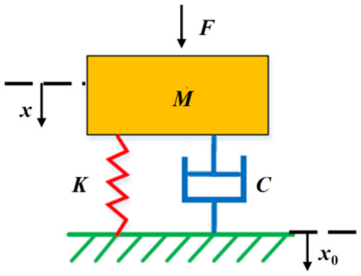

FIGURE 2. Equivalent model of the MVS.

In this paper, a novel compensation method is proposed based on the BP neural network under the TensorFlow architecture to compensate the temperature dependence of the MVS referring to Yu Ma et all's disturbance suppression method based on adaptive fuzzy neural network model [23]. The proposed compensation network is initially trained by feeding the amplitude and the frequency of the output voltage of the MVS, the temperature of the MVS, and the accuracy vibration amplitude of the excitation source. The well-designed weights and thresholds of the neural network can be therefore arrived at. And we can embed this algorithm into integrated devices to measure velocity excellently in real time [24], [25]. Finally, the effectiveness of the proposed method will be experimentally verified by measuring the detecting errors of the velocity under the temperature rise condition.

II. PROBLEM STATEMENT

The mechanical structure sketch of the MVS in this paper is shown in Fig. 1. The MVS is mainly composed of the permanent magnet, the coil, the support frame, and the spring. The dynamic system of the MVS can be simplified as a second-order system with single-degree-of-freedom, which if consisted of a mass M, a spring of stiffness K, and a damping C, as shown in Fig. 2.

The MVS converts the relative velocity of coil and permanent magnet into voltage signal proportional to the velocity based on the principle of electromagnetic induction.

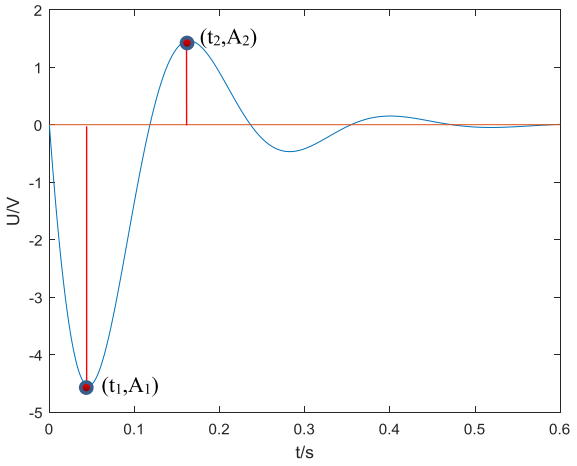

FIGURE 3. Second-order underdamped response curve.

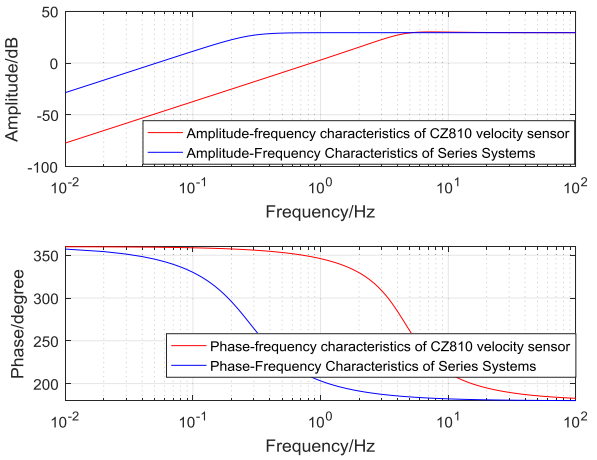

FIGURE 4. The Amplitude-Frequency characteristics before and after Expansion.

The induced electromotive force produced by the coil cutting the magnetic induction line is as follows:

$$e = WBlv\sin(\theta) = WBl(\dot{x}_1 - \dot{x}_0)\sin(\theta), \tag{1}$$

where W is the coil turn, B is the magnetic induction of permanent magnet (T), l is single-turn coil effective length (m), v is the relative velocity of coil and permanent magnet, θ is the angle between coil motion direction and magnetic field direction, $\dot{x}_1$ is absolute velocity of the coil, and $\dot{x}_0$ is absolute velocity of the permanent magnet.

The dynamic equation of the MVS can be written as,

$$M\ddot{x}_1 + f(\dot{x}_1 - \dot{x}_0) + K(x_1 - x_0) = F, \tag{2}$$

When the external force F= 0 acting on the measured object, the transfer function of the MVS can be deduced by deriving the Laplace transform of equations (1) and (2),

$$G_0(s) = \frac{U_0(s)}{V_0(s)} = \frac{-k_0 s^2}{s^2 + 2\zeta\omega_n s + \omega_n^2}, \tag{3}$$

where $\omega_n = \sqrt{k/m}$ is natural frequency, ζ is damping ratio, k_0 is sensitivity.

The natural frequency and the damping ratio of the MVS can be obtained by the direct current excitation method. A constant current is applied on the MVS, and the coil is suspended by the ampere force. Then, after the coil is stable, the constant current will be cut off instantaneously. The coil subsequently reaches the state of damped vibration. Since the coil cuts the magnetic induction line when it moves, the output of the MVS is a sinusoidal waveform whose amplitude decreases exponentially. The second-order underdamped curve can be measured as shown Fig. 3.

The natural frequency and damping ratio can be obtained by measuring the peak point coordinates of the response curve. The first peak point is (t1, A1) and second peak point is (t2, A2), then the natural frequency and damping ratio can be calculated by:

$$\zeta = \frac{\ln(A_1/A_2)}{\sqrt{\pi^2 + [\ln(A_1/A_2)]^2}}, \tag{4}$$

$$f_0 = \frac{1}{2|t_1 - t_2|\sqrt{1-\zeta^2}}, \tag{5}$$

The sweep frequency method is employed to acquire the natural frequency, the damping ratio, and the sensitivity of the MVS. The sinusoidal vibration signals with different frequencies are generated by an excitation source with a voice coil motor. The vibration signals are measured by both the standard velocity sensor and the MVS in this paper. The parameters of the MVS are as follows, the natural frequency $f_0 = 4.59$Hz, the damping ratio $\zeta_0 = 0.56$, and the sensitivity $K_0 = 29.14$V/m/s. Therefore, the transfer function of the MVS can be calculated as,

$$G_0(s) = \frac{-29.14s^2}{s^2 + 32.0851s + 831.2352}, \tag{6}$$

The compensation network can be therefore constructed according to the zero-pole compensation method, whose transfer function can be expressed as,

$$G_1(s) = \frac{s^2 + 32.0851s + 831.2352}{s^2 + 2.4876s + 3.0951}, \tag{7}$$

Based on the series compensation principle, the amplitude-frequency characteristics before and after expansion can be drawn based on equation (6) and (7), as shown in Fig. 4. As shown in Fig. 4, the zero-pole compensation method can expand the frequency band of the MVS. The bode diagrams of equations (6) and (7) can be sketched as Fig. 5.

However, when the temperature changes along with the external environment or long time running, the parameters of the MVS will change, which leads to equation (6) change. So the zero and pole points of equation (6) and (7) can't be cancelled by series connection. Then the second-order system will become a higher-order system, and the amplitude-frequency characteristics of the system deviate from the ideal value, which will cause the measurement error of the MVS.

In this paper, the temperature change of the MVS is measured by a K-type thermocouple as shown in Fig. 6. A sealed concrete structure without heat dissipation is constructed, which is consistent with the actual application. The varying

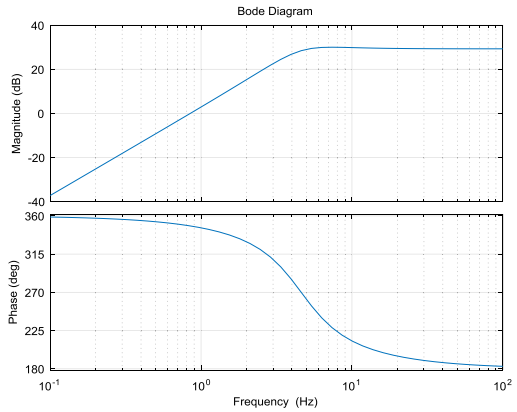

(a) Frequency characteristic curve of the MVS

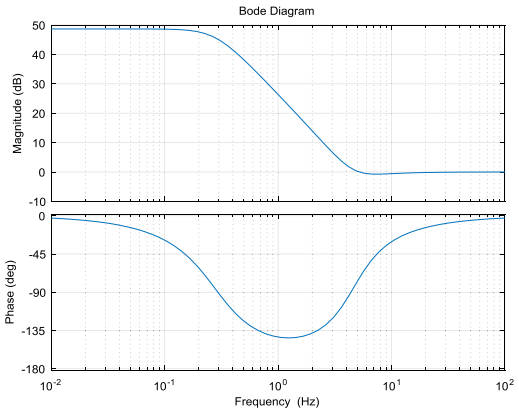

(b) Frequency characteristic curve of the compensation network

FIGURE 5. Frequency characteristic curve.

TABLE 1. Frequency characteristic curve.

Temperature (°C)	Neutral frequency (Hz)	Damping ratio	Sensitivity (V/m/s)
27.1	4.59	0.56	29.14
43.2	4.40	0.53	30.36
50.5	4.56	0.505	30.92
54.0	4.50	0.51	31.35
56.9	4.34	0.49	31.45
59.6	4.42	0.49	31.65

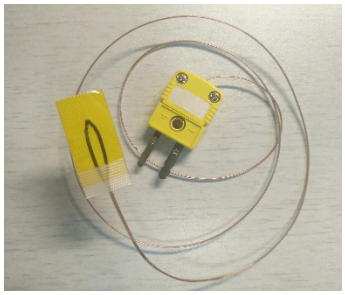

FIGURE 6. K-Thermocouple.

parameters of the MVS within 1hour are listed in Table 1. With the temperature increasing more than 30 °C, the sensitivity is increased by 2 V/m/s. The resolution of analog-to-digital conversion is 2mV. So the voltage corresponding to smallest vibration signal that can be measured is 2 mV. Velocity measurement deviation is 68.6um/s. The voltage corresponding to max vibration amplitude is about 0.073V. And velocity measurement deviation is 0.199mm/s, and the relative measurement deviation is 8%. The error is not ignored for nanoscale processing, for example, photolithography chip. With the same compensation network, the amplitude-frequency characteristic curve of the whole series system is shown in Fig. 7. It can be seen that the amplitude-frequency characteristics of the series system are greatly affected by temperature variation in the range of 0.5Hz to 10Hz near the natural frequency, so the measurement error of the vibration signal obviously occurs in this frequency range.

To solve the temperature dependency problem of the MVS, a dynamic compensation network should be adopted. The adaptive filtering based on the LMS is generally suitable for on-line identification of the system. But it is not suitable for the MVS because the ideal output signal is unknown during the measurement process. The Kalman filter does not need ideal output signal as a reference, which is generally applicable to the signal to be filtered including other noise signals. But the temperature variation causes the change of the system transfer function, so the Kalman filter is also unsuitable. A compensation method based on BP neural network under the TensorFlow architecture is proposed in this paper. The inputs of the proposed compensator are the amplitude, frequency of the output voltage, and the temperature of the MVS, the output of the compensator is vibration velocity. The parameters of the neural network can be obtained by the off-line training. MVS's voltage amplitude is connected with vibration velocity by sensitivity. The change of sensitivity is equivalent to the change of amplitude-frequency characteristic of MVS in Fig. 7, which is only related to frequency and temperature. So vibration velocity is decided by MVS's voltage amplitude, frequency and temperature. And we take above three variables as input nodes so as to reflect this information to the neutral network.

III. BP NEURAL NETWORK

A neural network is a mathematical algorithm model that processes distributed parallel information using a physical device to simulate the structure and function of a biological neural network. BP model is also called the multi-layer feed-forward network of errorback propagation algorithm. It is composed of multiple inputs and single output neurons connected according to certain topological structures; further, it studies through sample training, changes the weight value and threshold value of the internal connection such that the error between the output value and target value is minimal, and obtains a nonlinear mapping that can describe the relationship between the input and output of a system [26]–[28]. TensorFlow is a symbolic mathematical system based on data flow programming, which is widely used in the programming

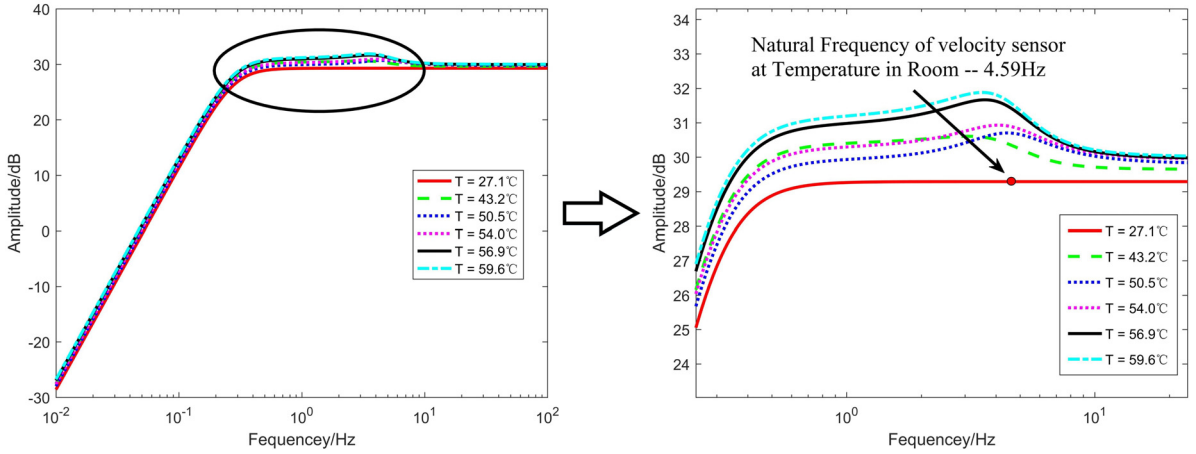

FIGURE 7. Amplitude-frequency characteristic curves with temperature variation.

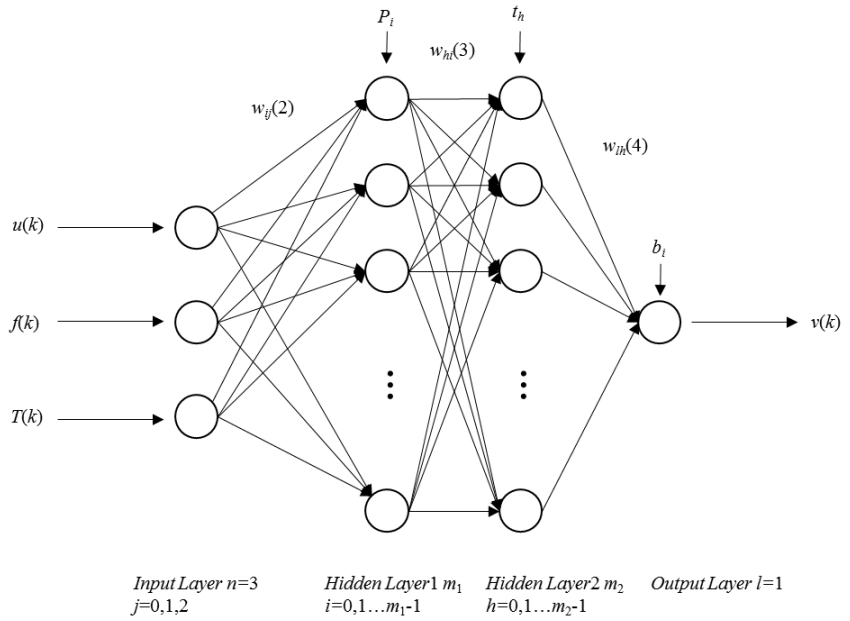

FIGURE 8. BP Neural Network model.

of various machine learning algorithms. Therefore, a BP neural network based on TensorFlow framework is built.

In this work, the BP model is consisted of one input layer, two hidden layers and one output layer, as shown in Fig. 8. The number of hidden layer and nodes in the hidden layer is determined by the actual training effect. In addition to the influence of temperature, the compensation effect is also affected by the amplitude and frequency of vibration signal, so the node of input layer is set to be 3. The activation function of hidden layer is a hyperbolic tangent function written by equation (8).

$$f_1(x) = \tanh(x) = \frac{2}{1+\exp(-2x)} - 1, \tag{8}$$

The activation function of the output layer is linear function written by equation (9).

$$f_2(x) = purelin(x) = x, \tag{9}$$

The index function is defined as equation (10).

$$J = \frac{1}{2}e^2(k) = \frac{1}{2}[y_c(k) - prediction(k)]^2, \tag{10}$$

where $y_c(k)$ is network training data, $prediction(k)$ is network prediction value and $e(k)$ is the deviation between actual value and prediction value.

The input layer nodes are shown in Fig. 8, which are the output voltage $u(k)$, frequency $f(k)$ of the compensated MVS, and the temperature $T(k)$ of the MVS. The output $O_j^{(1)}$ is also $u(k), f(k), T(k)$.

The input of the hidden layer is $O_j^{(1)}$, and the outputs are as follows.

$$net_i^{(2)}(k) = \sum_{j=0}^{2} w_{ij}^{(2)} O_j^{(1)}(k) + P_i, \tag{11}$$

$$O_i^{(2)} = f_1[net_i^{(2)}(k)], \quad i = 0, 1...m_1 - 1, \tag{12}$$

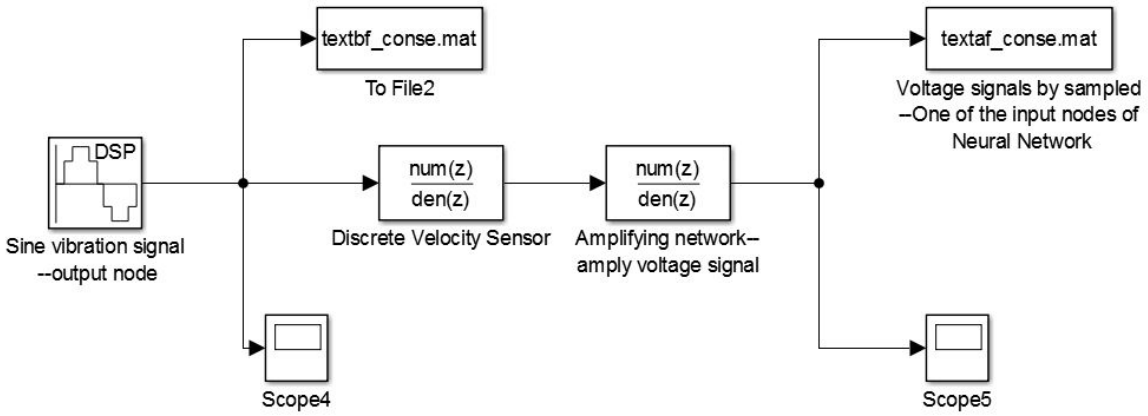

FIGURE 9. Simulation model.

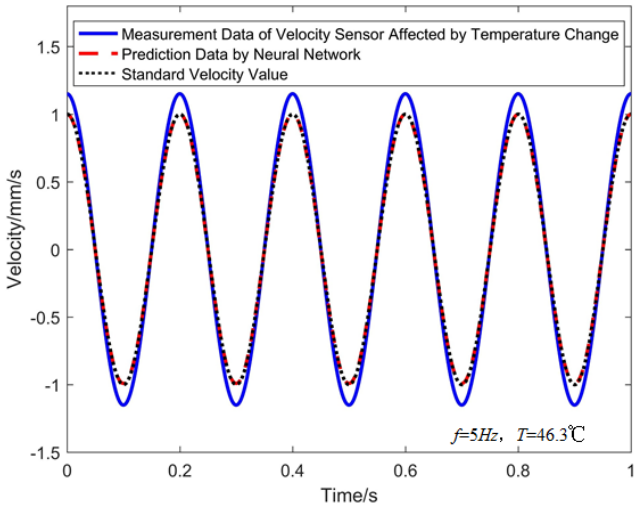

FIGURE 10. Neural network training effect.

$$net_h^{(3)}(k) = \sum_{i=0}^{m_1-1} w_{hi}^{(3)} O_i^{(2)}(k) + t_h, \tag{13}$$

$$O_h^{(3)} = f_1[net_h^{(3)}(k)], \quad i = 0, 1...m_2 - 1, \tag{14}$$

where $w_{ij}^{(2)}$ is the first hidden layer weight coefficient, $w_{hi}^{(3)}$ is the second hidden layer weight coefficient, P_i is the first hidden layer neuron threshold, t_h is the second hidden layer neuron threshold, $O_i^{(2)}$ is the output of the first hidden layer and $O_h^{(3)}$ is the output of the second hidden layer.

The outputs of the output layer are shown as equation (15) and (16).

$$net_l^{(4)}(k) = \sum_{i=0}^{m_2-1} w_{lh}^{(4)} O_h^{(3)}(k) + b_l, \tag{15}$$

$$O_l^{(4)} = f_2[net_l^{(4)}(k)], \quad l = 1, \tag{16}$$

Based on the index function (10), the gradient descent method is used to modify the weights of the network.

$$\Delta w_{ij}^{(2)} = -\eta \frac{\partial f_1}{\partial w_{ij}^{(2)}}, \tag{17}$$

$$\frac{\partial f_1}{\partial w_{ij}^{(2)}} = \frac{\partial f_1}{\partial y_c(k+1)} \cdot \frac{\partial y_c(k+1)}{\partial O_i^{(2)}} \cdot \frac{\partial O_i^{(2)}}{\partial net_i^{(2)}(k)} \cdot \frac{\partial net_i^{(2)}(k)}{\partial w_{ij}^{(2)}}, \tag{18}$$

where η is learning rate.

In the actual training process, the weights of each layer can be directly derived by the TensorFlow framework. Then the BP neural network can be realized by the embedded system with FPGA (Field Programmable Gate Array).

IV. SIMULATION

The simulation model is constructed in MATLAB/Simulink to validate the neural network compensator, as shown in Fig. 9. The transfer function of the MVS equation (6) and the compensation network equation (7) are discretized to Z-domain by the bilinear transformation. The compensation network in Fig.9 is to amplify the input signal below the cut-off frequency of the sensor and improve the signal-to-noise ratio (SNR), which can improve the fitting effect of the neural network. The inputs of the neural network compensator are amplitude and frequency of a sinusoidal signal which represents the vibration signal, and the temperature. The sample frequency is set to be 2kHz.

According to table 1, variation of sensor parameters including natural frequency, sensitivity, damping ratio, caused by variable temperature. So the discrete function of velocity sensor varies with temperature in Fig. 9. We use the actual measured parameters to reflect temperature dependence of velocity sensor. The temperature and sensor parameters are measured in actual experimental environment. Furthermore, the sine vibration signal of DSP module reflects actual vibration signal. Its frequency range is 0.5Hz-10Hz. And the vibration amplitude is consistent with the actual vibration amplitude measured by standard velocity sensor. So, the conditions for simulation experiments are comprehensive enough. It can reflect all possible situations in practical application.

As shown in Fig. 7, when the frequency of vibration signal is in the range of 0.5Hz to 10Hz, the MVS parameters change caused by temperature variation has the greatest impact on

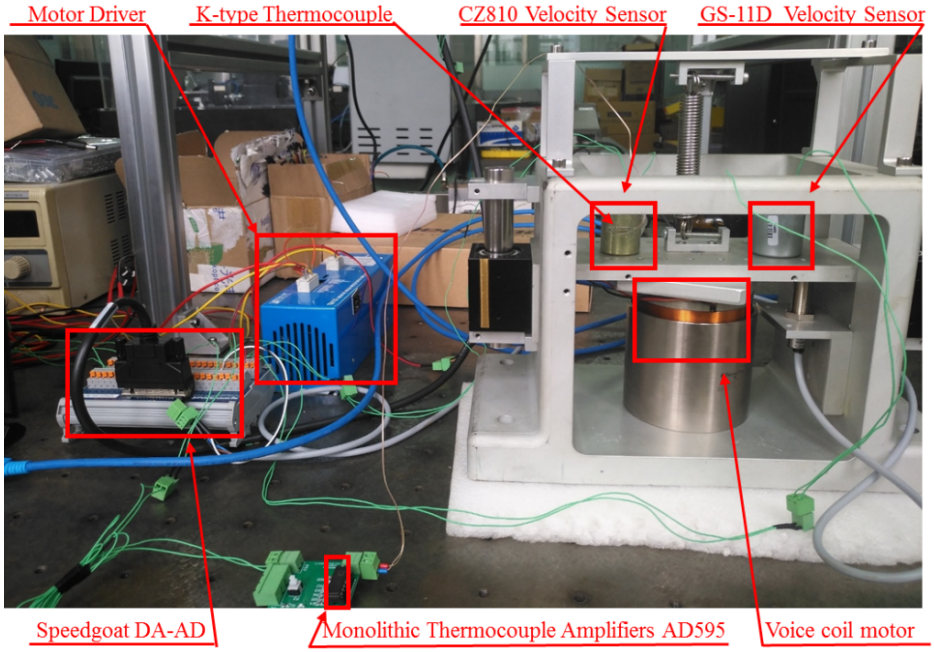

FIGURE 11. Experimental system.

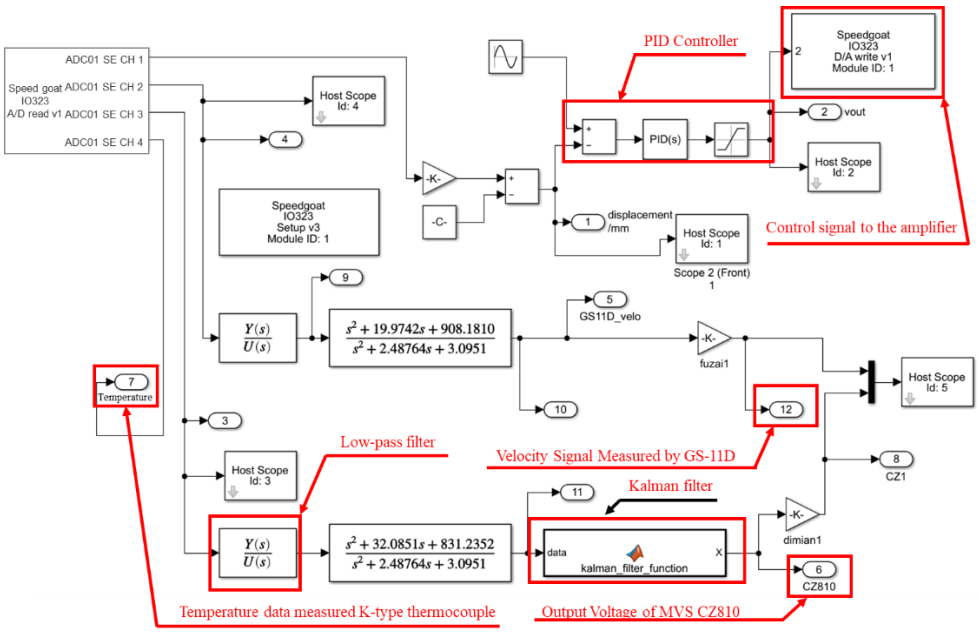

FIGURE 12. PID closed-loop control system block diagram for voice coil motor.

series compensation, so in the simulation, the amplitude of the input signal is set to be 0.5mm/s to 2.5mm/s, the frequency is set to be 0.5Hz to 10 Hz. According to Table 1, the temperature is set to be $T_0 = 27.1°C$, $T_1 = 43.2°C$, $T_2 = 50.5°C$, $T_3 = 54.0°C$, $T_4 = 56.9°C$ and $T_5 = 59.6°C$ which represent the temperature of MVS on different time. Then the training data of three input nodes and one output node is encapsulated.

The trained neural network is validated by a different vibration signal with amplitude 1mm/s, frequency 5Hz and temperature 46.3°C. The simulation result is shown in Fig.10. The output data of trained neural network is consistent with the actual velocity which is measured by the standard velocity sensor, and the measurement data from the MVS without compensation has obvious error which is affected by the temperature change.

V. EXPERIMENT

The experimental platform is shown in Fig. 11. A calibrated GS-11D velocity sensor severs as the standard sensor.

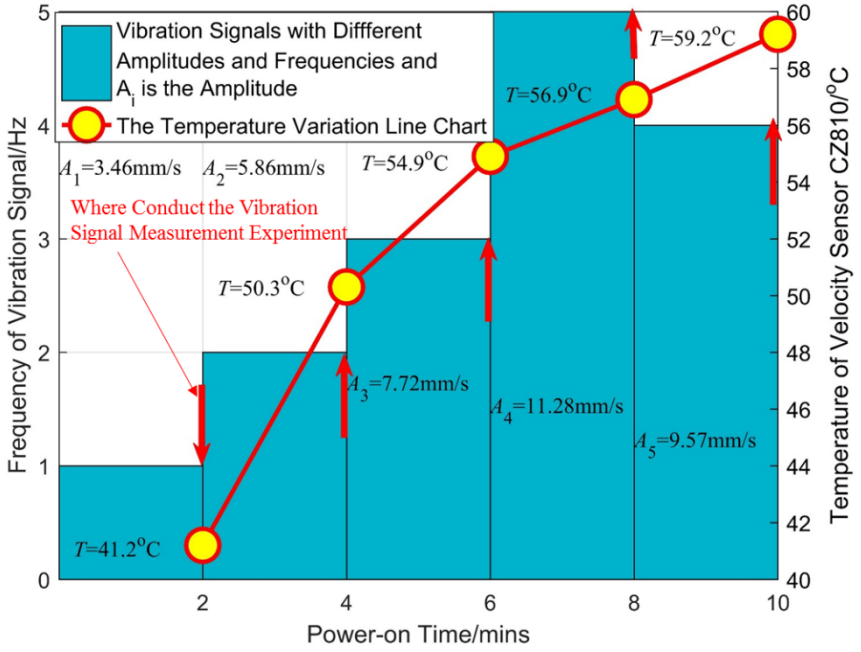

FIGURE 13. Experiment process. (a) The vibration with 1 Hz and 3.46 mm/s when *t* in [0, 2]; (b) the vibration with 2 Hz and 5.86 mm/s when *t* in (2, 4]; (c) the vibration with 3 Hz and 7.72 mm/s when *t* in (4, 6]; (d) the vibration with 5 Hz and 11.28 mm/s when *t* in (6, 8]; (3) the vibration with 4 Hz and 9.57 mm/s when *t* in (8, 10]. Temperatures are measured at 2, 4, 6, 8, and 10 minute.

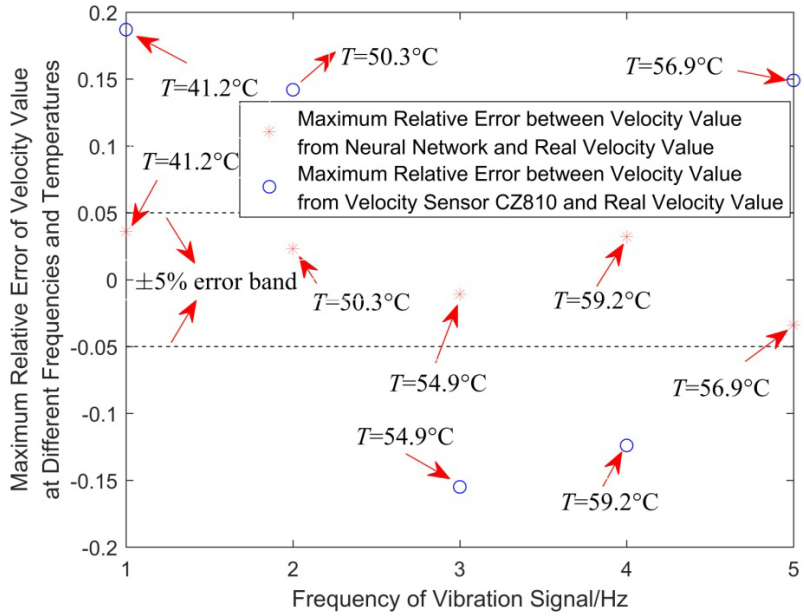

FIGURE 14. The maximum relative error of velocity measurements at different measuring points.

A K-type thermocouple is applied to measure the temperature of the CZ810 type MVS. The vibration signal is generated by a voice coil motor with a TA115 type amplifier. The whole experiment system is controlled by a Speedgoat Real-time system, which includes the PID closed-loop control module of the voice coil motor, the BP neural network compensator, and the sensor signal acquisition module. The software system is shown in Fig.12.

The frequency of vibration signal is adjusted from 0.5Hz to 10Hz with 0.1Hz interval, and the amplitude of vibration signal is adjusted from 0.5mm/s to 10mm/s with 0.1 mm/s interval. The output voltage and the temperature of the MVS, and the velocity measured by standard velocity sensor GS-11D are collected and packaged as training data of the BP neural network compensator under TensorFlow architecture. The Kalman filter shown

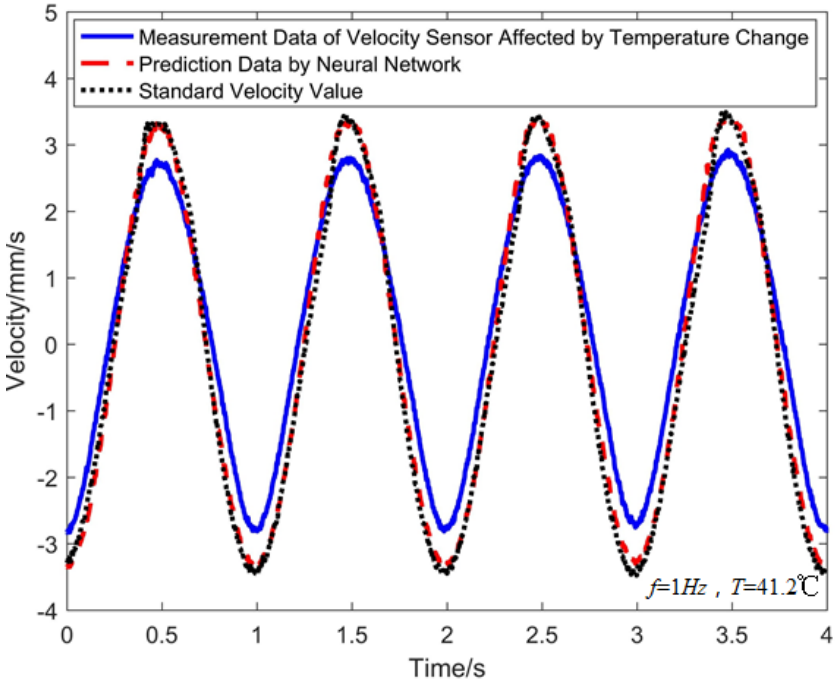

FIGURE 15. The measured time-domain vibration signal waveform when the vibration signal is 1Hz and the temperature of the sensor is 41.2 °C.

in Fig. 12 is designed to reduce the measurement noise based on the time update equations (19), (20) and the state update equations (21), (22) and (23).

$$\hat{x}_k^- = \hat{x}_{k-1} \tag{19}$$

$$P_k^- = P_{k-1} + Q \tag{20}$$

$$K_k = P_k^-/(P_k^- + R) \tag{21}$$

$$\hat{x}_k = \hat{x}_k^- + K_k(z_k - x_k^-) \tag{22}$$

$$P_k = (1 - K_k)P_k^- \tag{23}$$

where $\hat{x}_k \in R^n$ is n dimensional state variable, u_{k-1} is input control variable, $z_k \in R^m$ is m order observation variables, Q is covariance matrix of process excitation noise, R is covariance matrix of observation noise, K_k is Kalman gain and P_k is covariance matrix of state estimator error

Figure 13 indicates that a series of vibrations with varied frequencies and amplitudes are generated within 10 minutes. The temperature of the MVS greatly rises, which varies from 41.2 °C to 59.2 °C. As shown in Fig. 13, blue bars represent vibration signals with different amplitudes and frequencies and A_i represents the amplitude of vibration signal. Because the sample size is so large, only five groups of data are displayed here. The red arrows indicate where vibration signals are measured at a certain frequency. Taking 1Hz vibration signal for example, experiments are carried out at the frequency and temperature point when the time-period of applying DC voltage is 2 minutes, and that's to say the temperature of the sensor is 41.2 °C. Corroding to Fig. 7, the properties of the MVS varies with the temperature rise, which subsequently lead to the obvious measuring errors.

Figure 14 indicates that the maximum relative error of the MVS connecting with the proposed BP neural network is obviously reduced into the ±5% error band. National Standard (GB/T 6593-1996) regulates that the measurement results is eligible with high confidence probability if the relative error of measurement data is within 5% error band [29]. It is therefore experimentally verified that the proposed method is effective for compensating the temperature dependence of the MVS.

Fig. 15 shows that the measured time-domain vibration signal waveform when the vibration signal is 1Hz and the temperature of the sensor is 41.2 °C. The blue solid line represents the measured waveform of the velocity sensor CZ810, and the red dotted line represents the vibration velocity value compensated by the neural network. It can be seen that there is the big difference between the both, and the error between the latter and the true velocity value is even smaller. Fig. 15 indicates that the velocity value from the neural network compensator is in good agreement with the real velocity value in time-domain, that is, the phase delay is very small, so the velocity measurement value can be used for real-time feedback adjustment in low-frequency vibration isolation, thus realizing the real-time control system.

VI. DISCUSSION AND CONCLUSION

In this paper, a BP neural network dynamic compensator for the velocity sensor is established, which can effectively compensate the temperature dependence of the sensor and subsequently extend the detecting bandwidth and improve

the measurement accuracy. Experimental results indicate that the proposed compensator can keep the detecting errors of the velocity within ±5% error band, even though the temperature rise of the sensor has approximately reached 30 Celsius degrees. It is also experimentally verified that the minimum detecting frequency of the sensor can be extended to 0.28Hz from the natural 4.59Hz after applying the proposed compensator. In industrial practice, after deriving the coefficients of the neural network, the velocity signal can be measured by matrix operation with DSP or FPGA, and the vibration signal can be observed in real time with the host computer.

Therefore, the neural network compensator can replace the existing zero-pole compensation network and still has a good performance to measure low-frequency vibration signal even when the temperature changes. The proposed compensator is easily embedded into the integrated devices, which can be excellently applicable for the vibration isolation foundation applications.

REFERENCES

[1] H. Butler, "Position control in lithographic equipment [applications of control]," *IEEE Control Syst. Mag.*, vol. 31, no. 5, pp. 28–47, Oct. 2011.
[2] Y. R. Teo and A. J. Fleming, "Optimal integral force feedback for active vibration control," *J. Sound Vib.*, vol. 356, pp. 20–33, Nov. 2015.
[3] S. Ito, D. Neyer, S. Pirker, J. Steininger, and G. Schitter, "Atomic force microscopy using voice coil actuators for vibration isolation," in *Proc. IEEE Int. Conf. Adv. Intell. Mechatronics (AIM)*, Jul. 2015, pp. 470–475.
[4] N. Alujević, D. Čakmak, H. Wolf, and M. Jokić, "Passive and active vibration isolation systems using inerter," *J. Sound Vib.*, vol. 418, pp. 163–183, Mar. 2018.
[5] M. A. Beijen, D. Tjepkema, and J. van Dijk, "Two-sensor control in active vibration isolation using hard mounts," *Control Eng. Pract.*, vol. 26, pp. 82–90, May 2014.
[6] B. Yang and Y. Yang, "A new angular velocity sensor with ultrahigh resolution using magnetoelectric effect under the principle of Coriolis force," *Sens. Actuators A, Phys.*, vol. 238, pp. 234–239, Feb. 2016.
[7] K. Song, S. Tong, Z. Ding, and L. Dong, "An electromagnetic feedback method to improve low-frequency response performance of geophone," in *Proc. SENSORS*, Oct./Nov. 2016, pp. 1–3.
[8] M. Jafaripanah, B. M. Al-Hashimi, and N. M. White, "Application of analog adaptive filters for dynamic sensor compensation," *IEEE Trans. Instrum. Meas.*, vol. 54, no. 1, pp. 245–251, Feb. 2005.
[9] A. J. J. A. Oome, J. L. G. Janssen, L. Encica, E. Lomonova, and J. A. A. T. Dams, "Modeling of an electromagnetic geophone with passive magnetic spring," *Sens. Actuators A, Phys.*, vol. 153, no. 2, pp. 142–154, Aug. 2009.
[10] Y.-T. Lee, H.-D. Seo, A. Kawamura, T. Yamada, Y. Matsumoto, M. Ishida, and T. Nakamura, "Compensation method of offset and its temperature drift in silicon piezoresistive pressure sensor using double wheatstone-bridge configuration," in *Proc. Int. Conf. Solid-State Sens. Actuators*, Jun. 1995, pp. 570–573.
[11] T. Ishikawa, A. Nakayama, and H. Niimi, "Semiconductor ceramics having negative temperature coefficients of resistance," U.S. Patent 2001 0 001 205 A1, May 17, 2001. [Online]. Available: https://patentimages.storage.googleapis.com/b2/27/0a/0183f3f372ff3c/US20010001205A1.pdf
[12] K. Xiong and S. Wang, "Robust least mean logarithmic square adaptive filtering algorithms," *J. Franklin Inst.*, vol. 356, no. 1, pp. 654–674, Jan. 2019.
[13] Z. Dong, T. Bao, M. Zheng, X. Yang, L. Song, and Y. Mao, "Heading control of unmanned marine vehicles based on an improved robust adaptive fuzzy neural network control algorithm," *IEEE Access*, vol. 7, pp. 9704–9713, Jan. 2019.
[14] F. Huang, J. Zhang, and S. Zhang, "A family of robust adaptive filtering algorithms based on sigmoid cost," *Signal Process.*, vol. 149, pp. 179–192, Aug. 2018.
[15] M. Messini and M. Djendi, "A new adaptive filtering algorithm for stereophonic acoustic echo cancellation," *Appl. Acoust.*, vol. 146, pp. 345–354, Mar. 2019.
[16] Q. Zhang, "Adaptive Kalman filter for actuator fault diagnosis," *Automatica*, vol. 93, pp. 333–342, Jul. 2018.
[17] J. Wang, J. Wang, D. Zhang, X. Shao, and G. Chen, "Kalman filtering through the feedback adaption of prior error covariance," *Signal Process.*, vol. 152, pp. 47–53, Nov. 2018.
[18] C. Sang and M. Di Pierro, "Improving trading technical analysis with tensorflow long short-term memory (LSTM) neural network," *J. Finance Data Sci.*, vol. 5, no. 1, pp. 1–11, Mar. 2019.
[19] D. X. Zhou, "Universality of deep convolutional neural networks," in *Applied and Computational Harmonic Analysis*. London, U.K.: Elsevier, 2019. doi: 10.1016/j.acha.2019.06.004.
[20] W. L. Mao, "Recursive particle filter-based RBF network on time series prediction of measurement data," *Neural Process. Lett.*, vol. 50, pp. 1421–1449, Oct. 2019.
[21] L. Breiman, "Random forests," *Mach. Learn.*, vol. 45, no. 1, pp. 5–32, 2001.
[22] P. Xu *et al.*, "Temperature and humidity compensation for MOS gas sensor based on RandomForests," in *Intelligent Computing, Networked Control, and Their Engineering Applications*. Berlin, Germany: Springer, 2017, pp. 135–145.
[23] Y. Ma and Y. Cai, "A fuzzy model predictive control based upon adaptive neural network disturbance observer for a constrained hypersonic vehicle," *IEEE Access*, vol. 6, pp. 5927–5938, Mar. 2018.
[24] A. A. Hussain, N. Tayem, A.-H. Soliman, and R. M. Radaydeh, "FPGA-based hardware implementation of computationally efficient multi-source DOA estimation algorithms," *IEEE Access*, vol. 7, pp. 88845–88858, Jul. 2019.
[25] H. Phan-Xuan, T. Le-Tien, and S. Nguyen-Tan, "FPGA platform applied for facial expression recognition system using convolutional neural networks," *Procedia Comput. Sci.*, vol. 151, pp. 651–658, May 2019.
[26] Y. Xueshan, G. Feng, and H. Xingmin, "Low-frequency characteristics extension for vibration sensors," *Earthq. Eng. Eng. Vib.*, vol. 3, no. 1, pp. 139–146, 2004.
[27] B. Li, Y. Li, H. Wang, Y. Ma, Q. Hu, and F. Ge, "Compensation of automatic weighing error of belt weigher based on BP neural network," *Measurement*, vol. 129, pp. 625–632, Dec. 2018.
[28] J.-P. Zhang, P.-F. Gao, and F. Fang, "An ATPSO-BP neural network modeling and its application in mechanical property prediction," *Comput. Mater. Sci.*, vol. 163, pp. 262–266, Jun. 2019.
[29] *Quality Inspection Provisions for Electronic Measuring Instruments*, document GB/T 6593-1996, State Bureau of Technical Supervision, Standard Press of China, Beijing, China, 1996.